Field observations of basal forces and fluid pore pressure in a debris flow

Brian W. McArdell,[1] Perry Bartelt,[2] and Julia Kowalski[2]

Received 22 December 2006; revised 8 February 2007; accepted 23 February 2007; published 12 April 2007.

[1] Using results from an 8 m^2 instrumented force plate we describe field measurements of normal and shear stresses, and fluid pore pressure for a debris flow. The flow depth increased from 0.1 to 1 m within the first 12 s of flow front arrival, remained relatively constant until 100 s, and then gradually decreased to 0.5 m by 600 s. Normal and shear stresses and pore fluid pressure varied in-phase with the flow depth. Calculated bulk densities are ρ_b = 2000–2250 kg m^{-3} for the bulk flow and ρ_f = 1600–1750 kg m^{-3} for the fluid phase. The ratio of effective normal stress to shear stress yields a Coulomb basal friction angle of $\phi = 26°$ at the flow front. We did not find a strong correlation between the degree of agitation in the flow, estimated using the signal from a geophone on the force plate, and an assumed dynamic pore fluid pressure. Our data support the idea that excess pore-fluid pressures are long lived in debris flows and therefore contribute to their unusual mobility.
Citation: McArdell, B. W., P. Bartelt, and J. Kowalski (2007), Field observations of basal forces and fluid pore pressure in a debris flow, *Geophys. Res. Lett.*, *34*, L07406, doi:10.1029/2006GL029183.

1. Introduction

[2] Debris flows are rapid mass movements of mixed-size soil material and water that show flow behaviors intermediate between sediment-transporting floods and landslides [e.g., *Major et al.*, 2005; *Vallance*, 2005]. Interaction between the porous soil material and interstitial fluid are central to understanding the dynamics of debris flows [e.g., *Hutter et al.*, 1996; *Iverson*, 1997]. The presence of the fluid enhances the mobility of the solid phase through a variety of effects, including the reduction in the shear strength of the granular phase. Furthermore, large-scale laboratory experiments [*Iverson*, 1997; *Iverson and Vallance*, 2001; *Major and Iverson*, 1999] strongly support the hypothesis that pore fluid pressures larger than hydrostatic values are important in reducing the strength of the flowing material, thereby contributing to an explanation for the commonly long runout distances of debris flows.

[3] Coupled measurements of surface elevation and pore fluid pressure at the onset of failure [*Iverson et al.*, 1997] indicate that volume contraction at the onset of motion of a saturated mass results in pore fluid pressures in excess of hydrostatic values and a consequent reduction in shear strength. How long the excess pore fluid pressures persist in a moving mass is not yet generally known, although experiments by *Major and Iverson* [1999] suggest they persist until after deposition. Pore fluid pressures on the order of 50% larger than hydrostatic were observed in large-scale laboratory experiments on debris flows [*Iverson*, 1997, Figure 5b].

[4] Few field measurements of basal normal stress and pore fluid pressure during the flow are available. *Berti et al.* [1999] and *Berti and Simoni* [2005] report pore fluid pressure (up to 15–16 kPa) and total normal force (up to 12–14 kPa) data for one debris flow suggesting that the solid phase was carried completely in suspension at a distance of about 200 m from the initiation area. Herein we describe measurements of debris flow properties, including basal pore fluid pressure and normal and shear stresses, for a naturally-triggered debris flow observed four km downstream of its initiation.

2. Instrumentation and Field Observations

[5] The Illgraben catchment, in southwestern Switzerland, extends from the summit of the Illhorn mountain (elevation 2716 m a. s. l.) to the confluence of the Illbach river and the Rhone River (610 m a. s. l.) [*Hürlimann et al.*, 2003]. The catchment has an area of 8.9 km^2, but the sub-catchment susceptible to debris flow activity occupies 4.6 km^2. The geology is heterogeneous, composed of bands of quartzite, conglomerates, and calcareous sedimentary rocks on the southeast valley wall and massive cliff-forming dolomites on the northwest wall. Debris flows generally occur from May through October following convective rain storms. Flow initiation is probably related to sediment mobilization in areas where steep bedrock channels deliver large discharges of water on sediment deposits, similar to other debris flow-prone areas in the Alps [e.g., *Berti et al.*, 1999]. Most of the large blocks transported by debris flows, quartzite boulders up to several meters in diameter, are covered with percussion marks indicating vigorous collisions between particles.

[6] The channel on the alluvial fan has a U-shaped cross-section with base-widths of 5–10 m. Twenty-nine check dams are present over the distal 4.8 km of the channel and cause step-like vertical drops of up to several meters along the channel bed. The slope of the distal 2 km of channel decreases from 10 to 8% with local variations on the order of 7–18% persisting for ~50 m-long reaches.

[7] Instrumentation includes devices to measure front velocity, flow depth, and a force plate on the bed of the channel to measure normal and shear forces and fluid pressure. The average front velocity of a debris flow is determined using the travel time between a geophone sensor

[1]Swiss Federal Institute for Forest, Snow and Landscape Research, Birmensdorf, Switzerland.
[2]Swiss Federal Institute for Snow and Avalanche Research, Davos, Switzerland.

0094-8276/07/2006GL029183

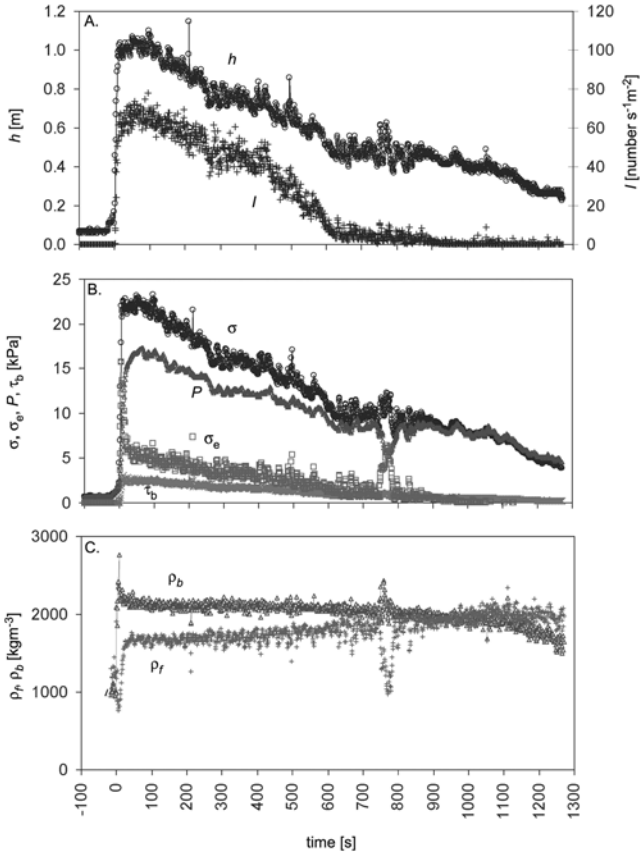

Figure 1. Data from the 2 August 2005 debris flow. (a) Flow depth and geophone signal, (b) measured stresses, and (c) calculated bulk mass densities. Time = 0 indicates the arrival of the debris flow front on the force plate.

installed on a concrete check dam [e.g., *Hürlimann et al.*, 2003] 460 m upstream of the force plate and a geophone mounted on the force plate. Flow depth is determined using a laser distance-measuring device mounted above the force plate. While the elevation of the surface of a debris flow may decrease somewhat, depending on the Froude number as the flow approaches the brink of the check dam, the bed cannot be eroded and little deposition occurs, thereby increasing the accuracy in comparison with less constrained reaches of the channel. Assuming that no sediment is deposited on the force plate, the flow depth is determined using the distance from the surface of the flow to the top of the force plate.

[8] The force plate is mounted horizontally at the crest of a concrete check dam with a trapezoidal shape (base width = 4.8 m). The force plate, installed flush with the channel bed, consists of a 2 m long (in the flow direction), 4 m wide, and 0.015 m thick steel plate, attached to an underlying steel frame which in turn rests on four corner-mounted vertical load cells. Two horizontal load cells are attached at the upstream end. The frame structure is acoustically insulated from the underlying check dam with stiff elastomer elements which provide overload protection for the sensors. The gap between the plate and surrounding concrete is a few mm wide and is sealed with a flexible silicon bead. Similar four-cell corner-mounted arrangements are commonly deployed for structural stability in industrial applications even though generally upon loading only three transducers respond at any given time. The transducer signals are sampled at 4 Hz, and the mean values per second are stored on a data logger.

[9] Basal pore fluid pressure is measured near the center of the force plate. A pressure transducer is mounted at the top of a closed sedimentation reservoir under the plate and is connected to the base of the flow via a short fiber-reinforced tube which is connected to a hollow mounting screw with an internal diameter of 8 mm; a steel plate is welded to the top of the mounting screw with a 2 mm diameter opening which is in contact with the base of the debris flow. The two-diameter reservoir entrance remained unclogged during the debris flow, unlike constant-diameter prototypes tested in 2004 or wire-mesh filters.

[10] A geophone measures vertical accelerations related to particle collisions on the force plate. We simplify the signal by recording the number of times per second that the voltage signal exceeds a small positive threshold value, thereby eliminating background noise. Under conditions of relatively low transport rate, as in gravel-bed rivers, this reduced signal corresponds approximately to the number of times that particles with a diameter larger than a few cm land on the sensor.

3. Results

[11] A debris flow on 2 August 2005 traveled with a front velocity $V_f = 1.4$ ms^{-1} over a nearly dry channel. While muddy water was always visible at the base of the flow front in video images, little water was visible in the gaps between boulders on the surface near the center of the flow until 10–20 s after the front had passed, indicating that a partially-saturated flow front [e.g., *Iverson and Vallance*, 2001] had a length of 15–30 m. After about 500 s boulders were visible only infrequently on the turbulent flow surface. Typical boulder sizes at the front and on the flow surface were 0.25 m. Video recordings indicate strong conveyor-belt-like circulation of particles. Boulders near the center and top of the flow moved at approx. $2V_f$ and were transported either to the lateral margins of the flow near the front where they traveled slower than the front, or to the front itself, where they were deposited and either buried (at the base of the front), or briefly rolled along the channel bed and then buried.

[12] After the event, the force plate was cleared of sediment and tare values for normal force, flow depth, and pore fluid pressure were obtained. For the horizontal force, the tare value was selected so that $\tau_b = 0$ before the arrival of the muddy pre-debris flow surge.

3.1. Field Data

[13] Following an initial pre-surge of muddy water, the flow depth increased from 0.1 to 1 m within 12 s of flow front arrival, remained relatively constant until approximately 100 s, and then gradually decreased to 0.5 m by 600 s (Figure 1a). Prominent peaks in the flow depth at 200 and 500 s correspond to the transport of unusually large boulders with diameters about the same dimension as the flow depth.

[14] Normal and shear stresses varied in-phase with flow depth (Figure 1b), with maximum values of $\sigma = 23$ kPa and

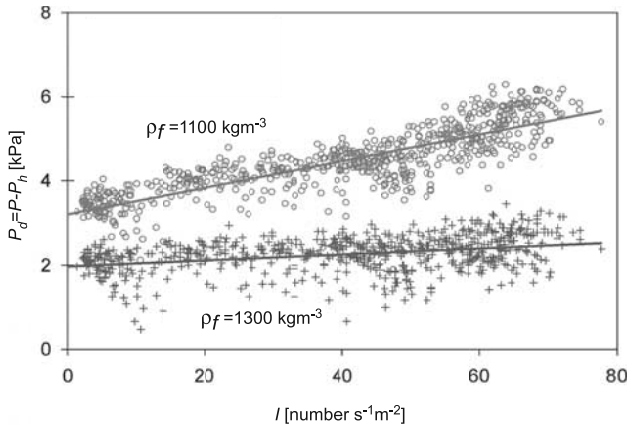

Figure 2. Dynamic pore fluid pressure P_d as a function of the number of impulses determined from the geophone signal I. The solid lines are least-squares regression lines fitted to the data.

τ_b = 2.8 kPa, respectively. We assume that the sediment (approx. 0.07 m thick) on the plate was removed with the arrival of the front. Shear stress values are on the order of 0.10σ. Although the steel plate is smoother than the stream bed upstream, no acceleration of the flow is apparent in the video recordings.

[15] Basal pore fluid pressure, P, (Figure 1b) increased linearly to 15 kPa at 15 s, followed by a more gradual increase to 17 kPa at 70 s. Subsequently, pore fluid pressure followed the same trend as the flow depth, with local peak values observed 0–5 s after corresponding peak values in the flow depth. Video recordings indicate that the fluid phase reached the upper surface of the flow at 10–20 s after passage of the front.

[16] The geophone data (Figure 1a) indicate a maximum number of impulses, I, corresponding to the maximum flow depth. However the signal decreases more rapidly after 400 s, eventually approaching zero, indicating lower concentrations of large-diameter sediment.

[17] Unexpected values from most sensors are observed at 750–800 s (Figure 1), which we interpret as temporary deposition of a large boulder along the edge of the force plate and a consequent diversion of flow. Unfortunately video recordings stopped at about 550 s.

3.2. Bulk Density

[18] The bulk density, ρ_b, of the flowing mixture can be calculated using the ratio of normal stress to flow depth above the force plate, $\rho_b = \sigma/(gh)$, where h is the flow depth and g is the acceleration due to gravity. Assuming that the depths of the fluid and solid phases are identical after 20 s, we calculate bulk mass densities for the entire flow ρ_b = 2000–2250 kg m^{-3} (Figure 1c). Large values in the two-second period near the front itself are likely caused by large vertical accelerations of individual particles as the front passes the plate and may be interpreted as the non-lithostatic pressures described by *Iverson* [1997]. The estimates of ρ_b are in a similar range as other debris flows [*Costa*, 1984; *Takahashi*, 1991; *Iverson*, 1997; *Major and Iverson*, 1999].

[19] Measured pore fluid pressure values can be used to constrain the bulk density of the fluid phase, which consists of water and fine sediment particles carried in suspension. Assuming that the height of the fluid phase is the same as the solid phase, the apparent average mass density of the fluid phase can be calculated using $\rho_f = P/(gh)$. Apparent pore fluid pressure densities are 1600–1750 kg m^{-3} (Figure 1c), somewhat larger than published estimates (1100–1300 kg m^{-3}, e.g., *Iverson* [1997]) suggesting that persistently large pore fluid pressures are present. Explanations for persistently large pore fluid pressures include: volumetric decreases in the space available for fluid due to a contraction in the volume of the material [*Iverson*, 1997], or dynamic pore pressures arising from the acceleration of the pore fluid as a result of granular collisions within the solid phase [*Hotta and Ohta*, 2000; *Iverson and LaHusen*, 1989; *Zenit and Hunt*, 1998]. Our geophone data coupled with pore-fluid pressure measurements allow us to investigate the second mechanism.

3.3. Dynamic Pore Fluid Pressure

[20] A dynamic pore-fluid pressure effect may be expected when a flow is in the grain-inertial regime where collisional stresses are important. The Savage number, modified for debris flows by *Iverson* [1997], can be used to assess if the flow is in the collisional flow regime:

$$N_{Sav} = \frac{\dot{\gamma}^2 \rho_s \delta}{N\left(\rho_s - \rho_f\right) g \tan\phi} \approx 10^{-6} - 10^{-1} \qquad (1)$$

where $\dot{\gamma}$ = shear rate, ρ_s = mass density of solid grains, ϕ = bulk friction angle, δ = characteristic grain size, and N = number of grains above layer of interest (the base of the flow in this case). A substantial proportion of the flow front surface is composed of large boulders, indicating that a large value of δ may be appropriate. If so, then N_{Sav} is close to a critical value of 0.1 indicating that the inertial stress created by grain collisions may be important and a dynamic pore pressure may be expected.

[21] Pore fluid pressure (measured) can be decomposed into the sum of a hydrostatic component and a dynamic component:

$$P = P_d + P_h \qquad (2)$$

where P_h is the hydrostatic pressure distribution, $P_h = \rho_f gh$, and P_d is an assumed dynamic component. Because the magnitude of P_d is unknown, we compare two plausible fluid densities to calculate P_h, ρ_f = 1100 and 1300 kg m^{-3}. Assuming that the number of impulses I is a surrogate for the degree of granular agitation in the flow, we expect the dynamic pressure, P_d, to increase with the number of impulses from the geophone signal, I. However the dependence of P_d on I is weak (Figure 2), suggesting that the dynamic pressure effect is small in this flow.

3.4. Basal Shear Stress and Basal Friction Angle

[22] Simultaneous measurements of total normal stress, σ, and pore fluid pressure, P, data allow us to calculate the effective normal stress, σ_e, at the base of the debris flow:

$$\sigma_e = \sigma - P. \qquad (3)$$

[23] Effective stress, σ_e, values (Figure 1b) are about 20% of the total normal stress over most of the duration of the

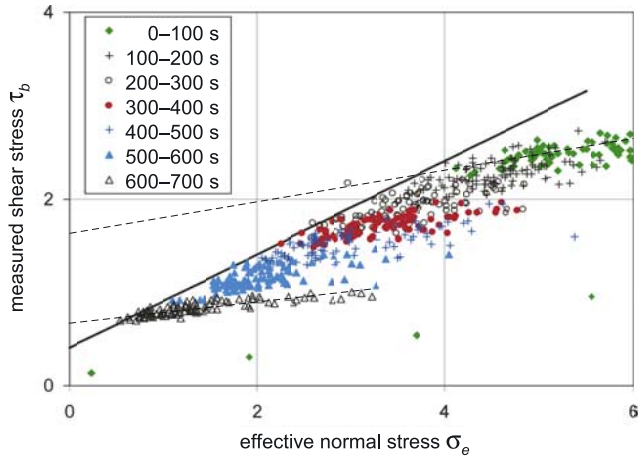

Figure 3. Measured shear stress as a function of effective normal stress. The data are divided into time intervals following the arrival of the debris flow front on the force plate. The solid line corresponds to the Coulomb basal friction angle of $\phi = 26°$. The two dashed lines schematically indicate the possibility of a retarding stress that decreases with time.

flow. The ratio of normal stress to fluid pressure gradually approaches a value of one, indicating that lithostatic pressures are reached in the fluid phase only after approximately 900 s even though excess pore fluid pressures are developed shortly after the arrival of the flow front.

[24] The relationship between the measured shear stress, τ_b, and effective stress, σ_e, may be described using a simple Mohr-Coulomb relationship:

$$\tau_b = c' + \sigma_e tan\phi_b' \quad (4)$$

where c' = the apparent cohesion, and ϕ_b' is the effective angle of basal friction. We find an apparent cohesion and friction angle of $c' = 0.45$ kPa and $\phi_b' = 26°$ (Figure 3). However the variation of properties along the flow wave indicates a more complex rheological behavior. We investigated the time-evolution of the normal-stress to shear-stress relationship by partitioning the flow into time periods near the front, middle, and tail of the wave. This analysis suggests the presence of a retarding stress (the intercept on the y-axis) that decreases along the wave from approx. 1.8 kPa near the front to 0.5 kPa at the tail, while the slope remains essentially constant (Figure 3). Because the experimental results indicate that the excess pore fluid pressures are persistent, a static Mohr-Coulomb relation is justified.

4. Conclusions

[25] Force and pore fluid pressure data collected during a debris flow traveling along a gently-sloping channel illuminate the importance of the role of pore fluid pressure in explaining the unusual mobility of debris flows in the field. Our results show that pore fluid pressures in excess of hydrostatic values are present over most of the duration of the flow supporting the idea that excess pore-fluid pressures are long lived in debris flows and therefore contribute to their unusual mobility. A correlation of an assumed dynamic pressure with geophone data suggest that a particle-collision-induced dynamic pore pressure effect, while most likely present in more rapidly sheared flows, may not be necessary to explain the large pore pressure values. A persistent mechanism that continually transfers the load from the solid phase onto the fluid phase must therefore exist. Additional observations of other debris flows are necessary to investigate this mechanism.

[26] **Acknowledgments.** We are grateful to B. Fritschi and F. Dufour for their contributions to the design and implementation of the Illgraben observation station and the force plate. Financial support from P. Greminger (BAFU) for the force plate and D. Bérod (Canton of Wallis, River Engineering Section) for the concrete constructions is appreciated. The support of A. Badoux, Ch. Graf, D. Rickenmann, and M. Swartz is appreciated. Two reviewers provided insightful comments that significantly improved the quality of the manuscript.

References

Berti, M., and A. Simoni (2005), Experimental evidences and numerical modeling of debris flow initiated by channel runoff, *Landslides*, *2*, 171–182.

Berti, M., R. Genevois, A. Simoni, and P. R. Tecca (1999), Field observations of a debris flow event in the Dolomites, *Geomorphology*, *29*, 265–274.

Costa, J. E. (1984), Physical geomorphology of debris flows, in *Developments and Applications in Geomorphology*, edited by J. E. Costa and P. J. Fleisher, pp. 268–317, Springer, New York.

Hotta, N., and T. Ohta (2000), Pore-water pressure of debris flows, *Phys. Chem. Earth, Part B*, *25*, 381–385.

Hürlimann, M., D. Rickenmann, and C. Graf (2003), Field and monitoring data of debris-flow events in the Swiss Alps, *Can. Geotech. J.*, *40*, 161–175.

Hutter, K., B. Svendsen, and D. Rickenmann (1996), Debris flow modeling: A review, *Continuum Mech. Thermodyn.*, *8*, 1–35.

Iverson, R. M. (1997), The physics of debris flows, *Rev. Geophys.*, *35*, 245–296.

Iverson, R. M., and R. G. LaHusen (1989), Dynamic pore-pressure fluctuations in rapidly shearing granular materials, *Science*, *246*, 796–799.

Iverson, R. M., and J. W. Vallance (2001), New views of granular mass flows, *Geology*, *29*, 115–118.

Iverson, R. M., M. E. Reid, and R. G. LaHusen (1997), Debris-flow mobilization from landslides, *Annu. Rev. Earth Planet. Sci.*, *25*, 85–138.

Major, J., and R. M. Iverson (1999), Debris-flow deposition: Effects of pore-fluid pressure and friction concentrated at flow margins, *Geol. Soc. Am. Bull.*, *110*, 1424–1434.

Major, J. J., T. C. Pierson, and K. M. Scott (2005), Debris flows at Mount St. Helens, Washington, USA, in *Debris Flow Hazards and Related Phenomena*, edited by M. Jakob and O. Hungr, pp. 685–731, Springer, New York.

Takahashi, T. (1991), *Debris Flow*, 165 pp., A. A. Balkema, Brookfield, Vt.

Vallance, J. W. (2005), Lahars, in *Debris Flow Hazards and Related Phenomena*, edited by M. Jakob and O. Hungr, pp. 247–274, Springer, New York.

Zenit, R., and M. L. Hunt (1998), The impulsive motion of a liquid resulting from a particle collision, *J. Fluid Mech.*, *375*, 345–361.

P. Bartelt and J. Kowalski, Swiss Federal Institute for Snow and Avalanche Research, Füelastrasse 11, CH-7260 Davos, Switzerland.

B. W. McArdell, Swiss Federal Institute for Forest, Snow and Landscape Research, Züercherstrasse 111, CH-8903 Birmensdorf, Switzerland. (mcardell@wsl.ch)